Journal of Inflammation Research

Dovepress
open access to scientific and medical research

Open Access Full Text Article

ORIGINAL RESEARCH

Angiotensin-(1–7) Analogue AVE0991 Modulates Astrocyte-Mediated Neuroinflammation via lncRNA SNHG14/miR-223-3p/NLRP3 Pathway and Offers Neuroprotection in a Transgenic Mouse Model of Alzheimer's Disease

Rui Duan[1,*]
Si-Yu Wang[1,*]
Bin Wei[1]
Yang Deng[2]
Xin-Xin Fu[2]
Peng-Yu Gong[1]
Yan E[1]
Xiao-Jin Sun[2]
Hai-Ming Cao[1]
Jian-Quan Shi[1]
Teng Jiang[1]
Ying-Dong Zhang[1,2]

[1]Department of Neurology, Nanjing First Hospital, Nanjing Medical University, Nanjing, 210006, People's Republic of China; [2]School of Basic Medicine and Clinical Pharmacy, China Pharmaceutical University, Nanjing, 211198, People's Republic of China

*These authors contributed equally to this work

Correspondence: Teng Jiang; Ying-Dong Zhang
Department of Neurology, Nanjing First Hospital, Nanjing Medical University, No. 68, Changle Road, Nanjing, Jiangsu, 210006, People's Republic of China
Email jiang_teng@njmu.edu.cn; zhangyingdong@njmu.edu.cn

Objective: Emerging evidence suggests that brain angiotensin-(1–7) (Ang-(1–7)) deficiency contributes to the pathogenesis of Alzheimer's disease (AD). Meanwhile, our previous studies revealed that restoration of brain Ang-(1–7) levels provided neuroprotection by inhibition of inflammatory responses during AD progress. However, the potential molecular mechanisms by which Ang-(1–7) modulates neuroinflammation remain unclear.

Materials and Methods: APP/PS1 mice were injected intraperitoneally with AVE0991 (a nonpeptide analogue of Ang-(1–7)) once a day for 30 consecutive days. Cognitive functions, neuronal and synaptic integrity, and inflammation-related markers were assessed. Since astrocytes played a crucial role in AD-related neuroinflammation whilst long noncoding RNAs (lncRNAs) were reported to participate in modulating inflammatory responses, astrocytes of APP/PS1 mice were isolated for high-throughput lncRNA sequencing to identify the most differentially expressed lncRNA following AVE0991 treatment. Afterward, the downstream pathways of this lncRNA in the anti-inflammatory action of AVE0991 were investigated using primary astrocytes.

Results: AVE0991 rescued spatial cognitive impairments and alleviated neuronal and synaptic damage in APP/PS1 mice. The levels of $A\beta_{1-42}$ in the brain of APP/PS1 mice were not affected by AVE0991. By employing high-throughput lncRNA sequencing, our in vitro study demonstrated for the first time that AVE0991 suppressed astrocytic NLRP3 inflammasome-mediated neuroinflammation via a lncRNA SNHG14-dependent manner. SNHG14 acted as a sponge of miR-223-3p while NLRP3 represented a direct target of miR-223-3p in astrocytes. In addition, miR-223-3p participated in the AVE0991-induced suppression of astrocytic NLRP3 inflammasome.

Conclusion: Our results suggest that Ang-(1–7) analogue AVE0991 inhibits astrocyte-mediated neuroinflammation via SNHG14/miR-223-3p/NLRP3 pathway and offers neuroprotection in APP/PS1 mice. These findings reveal the underlying mechanisms by which Ang-(1–7) inhibits neuroinflammation under AD condition and uncover the potential of its nonpeptide analogue AVE0991 in AD treatment.

Keywords: Alzheimer's disease, AVE0991, lncRNAs, SNHG14, miR-223-3p, astrocyte, neuroinflammation

Introduction

Alzheimer's disease (AD) is the most common cause of dementia in the elderly, affecting 5% of the population over 65 years.[1] Neuroinflammation, usually

Received: 15 October 2021
Accepted: 8 December 2021
Published: 18 December 2021

eliciting by amyloid-β (Aβ) accumulation, is considered as a neuropathological hallmark of AD.[2] Although moderate inflammatory response is essential for the brain to remove Aβ, chronic neuroinflammation may lead to the damage of neurons and synapses and subsequently deteriorates cognitive functions.[2] This notion was supported by previous observations that anti-inflammatory therapies effectively halt the disease progression in animal models of AD.[3]

The renin–angiotensin system (RAS) is an important modulator in the circulation system for the maintenance of sodium and water homeostasis.[4] Interestingly, emerging evidence suggests that RAS also exists in the brain and plays a crucial role in the pathogenesis of several neurological diseases including AD.[5] Ang-(1–7)/MAS1 axis is a recently identified axis of brain RAS.[6] As a heptapeptide, Ang-(1–7) is generated from Ang II by ACE2 and exerts beneficial effect via binding to MAS1 receptor.[7] Previously, we showed that Ang-(1–7) levels were decreased in the plasma of AD patients as well as the brain of AD mouse model.[8,9] Meanwhile, this reduction was correlated with the severity of neuropathology and cognitive functions.[10] These findings indicated that Ang-(1–7) deficiency might be involved in the pathogenesis of AD. More importantly, we and others revealed that restoration of brain Ang-(1–7) levels ameliorated chronic neuroinflammation and thus provided neuroprotection under AD context.[9,11] However, the potential mechanisms remain unclear so far.

Emerging evidence indicates that astrocyte plays a crucial role in AD-related neuroinflammation.[12] Meanwhile, MAS1 receptor was reported to be highly expressed on astrocytes.[13] In addition, as a subgroup of noncoding RNAs (ncRNA), long noncoding RNAs (lncRNAs) were revealed to participate in modulating neuroinflammation.[14] Interestingly, recent studies also uncovered a close interaction between Ang-(1–7)/MAS1 axis and several lncRNAs.[15,16] In view of this evidence, we employed primary astrocytes and APP/PS1 mice to investigate whether lncRNAs were involved in the anti-inflammatory action of Ang-(1–7) during AD progression. It should be noted that Ang-(1–7) has a relatively short duration of biological effect in vivo since it can be rapidly inactivated and degraded by several proteases.[17] To avoid this disadvantage, a nonpeptide Ang-(1–7) analogue AVE0991 was used in the subsequent experiments.

Methods

Animals

Male APP/PS1 transgenic mice (7-month-old) and their age-matched wild-type (WT) mice were obtained from Beijing Zhishan Co., Ltd. According to our previous observations, AD-related neuroinflammation and spatial cognitive impairments become apparent at this age.[18] Mice were housed in a regulated environment (23±1 °C, 60±5% humidity) with a 12 h light/12 h dark cycle. This study was approved by the Animal Care and Use Committee of Nanjing First Hospital, Nanjing Medical University (Approval #: IACUC-1911032). All animal experiments were conducted in accordance with the ethical standards of Nanjing First Hospital.

Drug Administration

Mice were injected intraperitoneally with vehicle (0.9% sterile saline) or AVE0991 (a nonpeptide Ang-(1–7) analogue, 10 mg/kg, MedChemExpress LLC, Monmouth Junction, NJ, USA) once a day for 30 consecutive days (see Supplementary Figure S1). The dose and route of AVE0991 administration were chosen based on previous studies.[9,19] According to our previous findings, AVE0991 could steadily cross the blood–brain barrier via intraperitoneal injection route.[9,19] During the whole experiment, we monitored the general health of mice and did not observe obvious adverse effects or significant changes in their body weight or food intakes. Additionally, systolic blood pressure (SBP) was measured at the beginning and the end of the treatment period using a tail-cuff method as described.[19] AVE0991 injection (10 mg/kg/day) did not significantly affect SBP of APP/PS1 mice at the end of the treatment period (106.27±19.09 mmHg vs 102.44 ±11.67 mmHg, $P>0.05$).

For cell experiment, AVE0991 was diluted in DMEM/F12 (Gibco, Armonk, NY, USA) to achieve a final concentration at 10 μM. Oligomeric $A\beta_{1-42}$ (Abcam, Inc., MA, USA) was prepared as described,[18,20] and diluted with DMEM/F12 to a final concentration of 5 μM. The dose of AVE0991 and $A\beta_{1-42}$ in cell experiments was chosen based on previous studies.[9,18]

Morris Water Maze (MWM)

The MWM test was used to evaluate spatial learning and memory through an Ethovision 3.0 video tracking system (Noldus Information Technology B.V., Wageningen, Netherlands). Briefly, a hidden round platform (10 cm

diameter) was placed 1 cm below the water surface (located in the center of the southwest quadrant of a circular pool). Mice were trained for 5 consecutive days with 4 trials per day. The mice were given 60 seconds to locate the platform, If the mice cannot locate the platform within 60 seconds, they were guided to the platform and remained for another 15 seconds. One day after the last trial, the hidden round platform was removed, and a probe test was performed. The path length to the submerged platform was recorded, and the average value of four trials was calculated.

Western Blot

Mice whole brains or primary astrocytes were homogenized in cold RIPA buffer and centrifuged at 4°C at 12,000 g for 10 min. A bicinchoninic acid protein assay kit (Thermo Fisher, Waltham, MA, USA) determined the concentration of protein in the supernatants. Protein samples of 30 μg were separated by sodium dodecyl sulfate polyacrylamide gel electrophoresis and transferred to polyvinylidene fluoride membranes. A tris buffered saline of 10% non-fat dried milk blocked membranes for 1 h and incubated with primary antibodies (rabbit anti-NLRP3 (1:1000; #15101, Cell Signaling Technology, Danvers, MA, USA) or rabbit anti-synaptophysin monoclonal (1:1000; #4329, Cell Signaling Technology)). The anti-β actin (1:1000; #4970, Cell Signaling Technology) was used as a loading control. Membranes were incubated with goat anti-rabbit (1:5000; #7074, Cell Signaling Technology) secondary antibodies at room temperature for 2 h. Immune complexes were assessed with peroxidase and an enhanced chemiluminescence system (Thermo Fisher, USA). The Western blot band densities were quantified by Quantity one software (BioRad, CA, USA).

Nissl Staining

Nissl staining was conducted as described.[11] The whole brains fixed with 4% paraformaldehyde were embedded in paraffin and cut into 4-μm-thick sections. The sections were treated with Nissl staining solution for 5 min. Neurons with dark violet nucleus and intact morphology were identified as Nissl-positive neurons. Two coronal sections at different depths on the rostrocaudal axis (−1.5 mm, and −2.5 mm from bregma) were imaged for each mouse. Three fields of hippocampus CA1 subregions on each coronal section were then randomly selected, and the percentage of Nissl-positive neurons were calculated using Image-Pro Plus 7.0 by observers who were unaware of the experimental groups.

ELISA

For measuring the brain levels of tumor necrosis factor-α (TNF-α), interleukin-6 (IL-6) and interleukin-1β (IL-1β), the whole brains were homogenized in 0.9% saline. For assessing the medium levels of IL-1β, the supernatant medium of primary astrocytes was collected. The homogenates or the collected supernatant medium was centrifuged at 12,000 rpm for 20 min. The supernatants were then collected and stored at −80°C. The concentrations of TNF-α (#MTA00B, R&D Systems, Inc., Minneapolis, MN, USA), IL-6 (#M6000B, R&D Systems, Inc.) and IL-1β (#MLB00C, R&D Systems, Inc.) were analyzed using commercial ELISA kits according to the manufacturer's instructions. The final levels of these cytokines were determined according to the standard curve of absorbance.

Quantitative Real-Time Polymerase Chain Reaction (qRT-PCR) Analysis

Whole brains or astrocytes were homogenized and dissolved in Trizol (Invitrogen, Carlsbad, CA, USA) to extract RNA. The concentrations of RNA were measured by a Nanodrop 2000 spectrophotometer (Thermo Fisher, USA). Reverse transcription was performed using a cDNA Synthesis Supermix (TAKARA, Kusatsu, Shiga, Japan). The cDNA was subjected to qRT-PCR with the SYBR qPCR Supermix Plus (TAKARA). Expression data were normalized to β-actin. In addition, the total RNA was reverse transcribed to determine the miRNA expression, and the resulting cDNA was mixed with miRNA-specific TaqMan primers (springen, Nanjing, China) and TaqMan Universal PCR Master Mix (TAKARA). U6 RNA was used as an endogenous control for data normalization. Relative changes in expression were measured using the comparative threshold cycle (Ct) method and 2-ΔΔCt as described,[21] and the results indicated the fold change of expression. These primers for qRT-PCR are shown in Supplementary Table S1.

Isolation of Adult Astrocytes

Adult Brain Dissociation Kit and ACSA-2 MicroBeads (Miltenyi Biotec, Bergisch Gladbach, Germany) were used for magnetic isolation of astrocytes from 8-month-old APP/PS1 (with or without AVE0991 treatment) mice and their age-matched WT controls. Adult Brain

Dissociation Kit was used to digest the brain and prepare single-cell suspension. Then, debris and red blood cells were removed. Astrocytes were incubated for 15 min at 4°C with ACSA-2 MicroBeads and separated from single-cell suspension in a magnetic field using MS columns, MACS MultiStand and QuadroMACS (Miltenyi Biotec).

LncRNA Sequencing

RNA was extracted from adult astrocytes using Trizol (Invitrogen) according to the manual instructions. After removing the ribosomal RNA, the RNA library was prepared. RNA sequencing was performed on a MGISEQ-2000 System (BGI, Shenzhen, China). After the raw data were trimmed and filtered, the remaining data were then mapped using HISAT2 v2.0.4.[22] Differential lncRNA expression was evaluated using DESeq2 v1.4.5.[23] The significant levels were corrected by Q value with a rigorous threshold by Bonferroni. The sequencing data have been deposited in GenBank (GSE184967).

Primary Astrocytes Culture

The whole brains of postnatal 1-day-old C57Bl/6 mice were chopped and mechanically minced using a 70-μm nylon mesh. The mixed cells were seeded in 75T flasks and grown in DMEM/F12 supplemented with 10% FBS, 100 unit/mL penicillin, and 100 μg/mL streptomycin. Mixed glial cultures were maintained in a 5% CO_2 incubator at 37°C for 2 weeks. To obtain primary astrocytes, 75T flasks containing mixed glial cells were sealed with foil and shaken at 250 rpm on a rotary shaker at room temperature overnight. The culture medium was then discarded, and the cells were dissociated using trypsin-ethylene diamine tetraacetic acid and centrifuged at 2000 rpm for 30 min. After centrifugation, the pellet (primary astrocytes) was collected and used for experiments.

CRISPR-dCAS9-SAM Lentivirus Transduction

GV468-SNHG14 lentivirus and dCAS9-VP64-Puro lentivirus were obtained commercially from GeneChem (Shanghai, China). They were applied to astrocytes in the presence of 5 μg/mL polybrene for 48 h. SNHG14-overexpressing cells were then selected using puromycin (5 μg/mL).

Fluorescent in situ Hybridization (FISH)

SNHG14 probes (5′-CAAATCAACATTCCAGTCTCT ATCTA-3′) were purchased from RiboBio Co., Ltd (Guangzhou, China). For in situ hybridization in frozen brain slices, mice were perfused with phosphate-buffered saline (PBS) and 4% paraformaldehyde solution in PBS. The brain tissues were fixed in 4% paraformaldehyde solution in PBS overnight at 4°C and subsequently cryoprotected in 30% sucrose in PBS overnight at 4°C. Afterward, they were cryosectioned at 16 mm thickness. Probes were diluted to 1:50, and the in situ hybridization was performed according to the manufacturer's protocol. After completion of the in situ hybridization, brain slices were blocked for 1 h in blocking buffer. The slices were stained overnight at 4°C using rabbit anti-GFAP (1:200; #80788, Cell Signaling Technology), washed 3 times with PBS, and incubated with Anti-rabbit IgG (1:400; #4414, Cell Signaling Technology) for 1 h at room temperature. 4′,6-Diamidino-2-phenylindole was used to visualize nuclei. Slices were then mounted for microscopy.

Transient Transfection

As described,[24] primary astrocytes were plated onto 6-well plates. When cells were reaching about 70% confluence, lipofectamine 2000 (Invitrogen) was used to carry out the transient transfection of siRNA, miRNA mimics or miRNA inhibitor. The transfection reagent complexes containing 50 nM siRNA, 100 nM miRNA mimics or 100nM miRNA inhibitor were added to each well and then incubated at 37 °C for 6 h. Then, the cell culture was replaced by fresh DMEM/F-12 with 10% FBS. The siRNA, miRNA mimics and miRNA inhibitor sequences were shown in Supplementary Table S2.

Luciferase Reporter Assays

The potential miR-223-3p binding sites in SNHG14 were predicted using RNAhybrid (http://bibiserv2.cebitec.uni-bielefeld.de/rnahybrid). The WT SNHG14 sequence and its mutant (Mut, only the putative miR-223-3p binding sites were mutated) were synthesized and cloned into vector psiCHECK-2 (Promega, Madison, WI, USA), respectively. Then, we utilized TargetScan 7.2 online prediction software (http://www.targetscan.org/vert_72/) to screen the potential miRNAs that could bind to 3′-UTR sequence of NLRP3 and predicted the binding sites between NLRP3 and miR-223-3p. The basic information and species conservativeness of SNHG14 and miR-223-3p were obtained from the UCSC Genome Bioinformatics

website (http://genome.ucsc.edu/). The WT or the Mut of NLRP3 3′-UTR or SNHG14 luciferase reporter constructs were co-transfected into HEK 293T cells with miR-223-3p mimic or NC mimic using lipofectamine 2000. After 48 h of transfection, the cells were collected and examined with a dual-luciferase reporter assay system (Promega, Wisconsin, USA).

Statistical Analysis

Data are represented as mean ± standard deviation (SD). The statistical analyses were carried out by using GraphPad Prism 8 (GraphPad Software, Inc., La Jolla, USA). Student's *t*-test was used for the comparison between two groups. One-way ANOVA followed by Tukey's post hoc test was employed to analyze differences among three or more groups. MWM data were analyzed by two-way repeated measures ANOVA followed by Bonferroni's multiple comparisons test. $P<0.05$ was considered statistically significant.

Results

AVE0991 Rescues Cognitive Impairments and Offers Neuroprotection in APP/PS1 Mice

MWM test was conducted during the last 6 days before animals were sacrificed. As demonstrated by Figure 1A, no difference was noted in swimming speed between APP/PS1 mice and their age-matched WT controls. Injection of AVE0991 did not significantly influence swimming speed in APP/PS1 mice (Figure 1A) or their age-matched WT controls. We then employed a hidden platform test to evaluate the spatial learning performance in APP/PS1 mice and their age-matched WT controls. As revealed by Figure 1B, APP/PS1 mice performed worse than their age-matched controls during the test ($F_{genotype}$ (1, 110)=22.13, $P<0.05$), indicating that APP/PS1 mice exhibited evident spatial learning impairments at 8 months of age. AVE0991 injection rescued this spatial learning impairments in APP/PS1 mice (Figure 1B, $F_{treatment}$ (1, 110)=11.70, $P<0.05$). Afterwards, probe test was carried out. As shown by Figure 1C, APP/PS1 mice spent less time in the target quadrant when compared with WT controls ($P<0.05$), indicating evident spatial memory impairments. AVE0991 treatment recovered this spatial memory impairments in APP/PS1 mice (Figure 1C, $P<0.05$). It should be noted that injection of AVE0991 had no influence on spatial cognitive functions in WT controls (See Supplementary Figure S2).

As shown by Figure 1D and E, APP/PS1 mice displayed apparent hippocampal synaptic loss (indicated by synaptophysin protein levels) when compared with their age-matched WT controls ($P<0.05$). Meanwhile, an obvious neuronal loss (indicated by Nissl-positive neurons) in the hippocampus was also observed in the brain of APP/PS1 mice (Figure 1F and G, $P<0.05$). As indicated by Figure 1D and E, AVE0991 injection led to a significant increase in synaptophysin protein levels ($P<0.05$). Meanwhile, the percentage of Nissl-positive neurons in the hippocampus was significantly elevated after AVE0991 treatment (Figure 1F and G, $P<0.05$). Injection of AVE0991 had no impact on the synaptophysin protein levels or the percentage of Nissl-positive neurons in the brain of WT controls (data not shown).

AVE0991 Does Not Influence $A\beta_{1\text{-}42}$ Levels in the Brain of APP/PS1 Mice

As indicated by Supplementary Figure S3, AVE0991 treatment slightly decreased the levels of $A\beta_{1\text{-}42}$ in the brain of APP/PS1 mice, but the difference did not reach statistical significance.

AVE0991 Suppresses Neuroinflammation in APP/PS1 Mice

As revealed by Figure 2A–C, APP/PS1 mice showed higher protein levels of pro-inflammatory cytokines including IL-1β, IL-6 and TNF-α in the brain when compared with their age-matched WT controls. AVE0991 treatment markedly reduced the protein levels of IL-1β, IL-6 and TNF-α in the brain of APP/PS1 mice (Figure 2A–C).

LncRNA SNHG14 May Be Involved in the AVE0991-Induced Inhibition of Astrocytic NLRP3 Inflammasome

Astrocyte played a crucial regulating role in AD-related neuroinflammation whilst MAS1 receptor is highly expressed on astrocytes.[12,13] Meanwhile, NLRP3 inflammasome was identified within astrocytes, and activation of NLRP3 inflammasome elicits neuroinflammation during AD progression.[25,26] Therefore, we isolated astrocytes from 8-month-old APP/PS1 mice with or without AVE0991 treatment to investigate whether suppression of astrocytic NLRP3 inflammasome was involved in the anti-

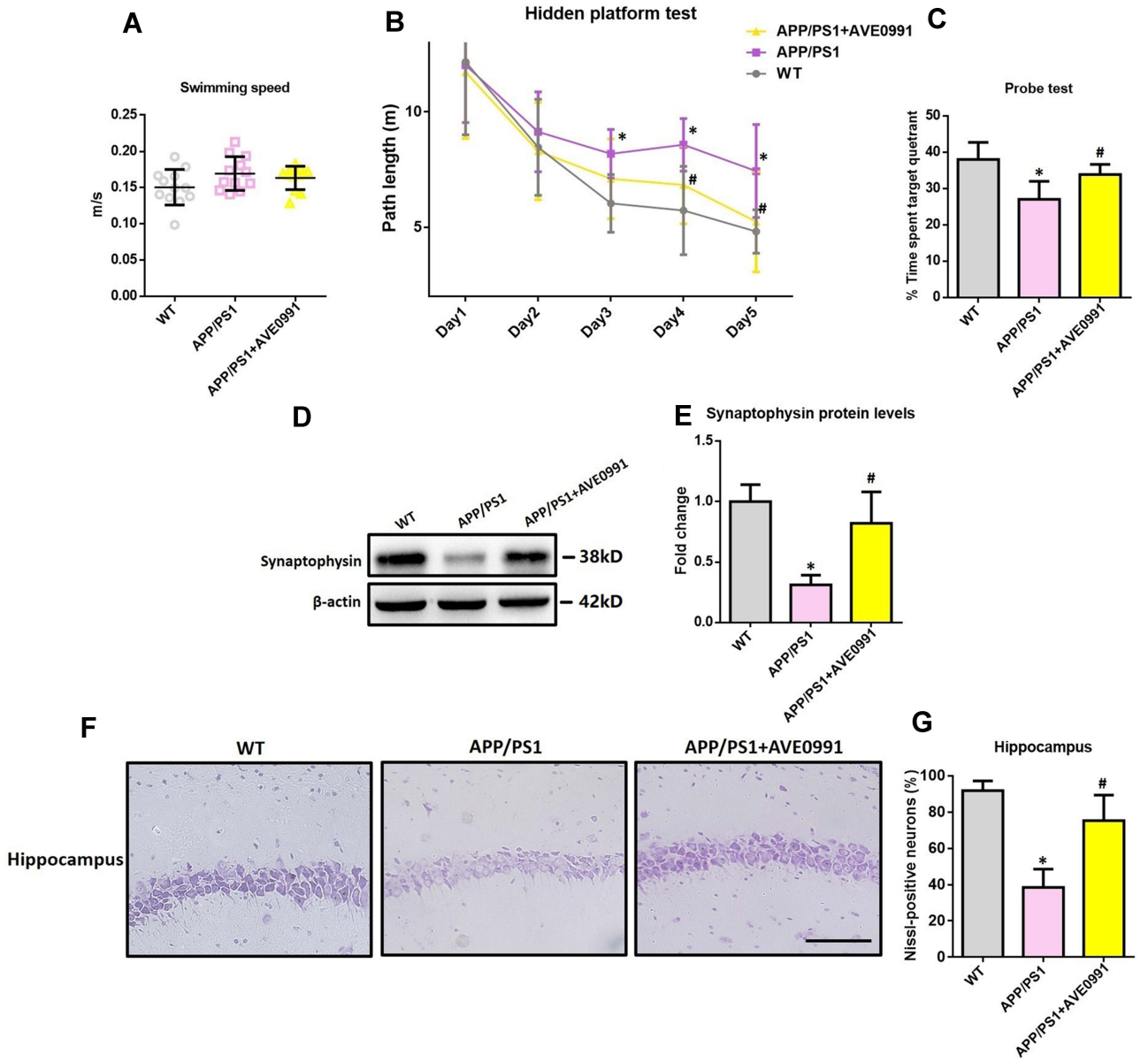

Figure 1 AVE0991 rescues cognitive impairments and offers neuroprotection in APP/PS1 mice. (**A**) Swimming speed of each group in the Morris water-maze test (n=12 per group). (**B**) Path length of each group in the hidden platform test (n=12 per group). (**C**) The percentage of time spent in the target quadrant in the probe test ((n=12 per group). (**D** and **E**) Representative Western blot bands and densitometric analysis of synaptophysin in the brain. β-Actin was used as an internal control (n=6 per group). (**F**) Neuronal loss in the hippocampus of mice was detected by Nissl staining. Neurons with dark violet nucleus and intact morphology were identified as Nissl-positive neurons. Scale bar=100 μm (n=6 per group). (**G**) Quantitative analysis of Nissl-positive neurons in the brain (n=6 per group). All data are expressed as the mean ± SD. **P*<0.05 versus the WT group. #*P*<0.05 versus the APP/PS1 group.

inflammatory actions of AVE0991. As demonstrated by Figure 3A and B, astrocytes from APP/PS1 mice without AVE0991 treatment displayed a significantly higher protein levels of NLRP3 when compared with those from age-matched WT controls, indicating activation of NLRP3 inflammasome in astrocytes under AD condition. Astrocytes from AVE0991-treated APP/PS1 mice exhibited a significant reduction in NLRP3 protein levels (Figure 3A and B), indicating a suppression of NLRP3 inflammasome in astrocytes following AVE0991 treatment.

LncRNAs were reported to participate in modulating neuroinflammation.[14] To test whether lncRNAs were involved in the AVE0991-induced inhibition of astrocytic NLRP3 inflammasome, we performed high-throughput lncRNA sequencing in primary astrocytes from APP/PS1 mice with or without AVE0991 treatment. As revealed by Figure 3C, a total of 31 differentially expressed lncRNAs

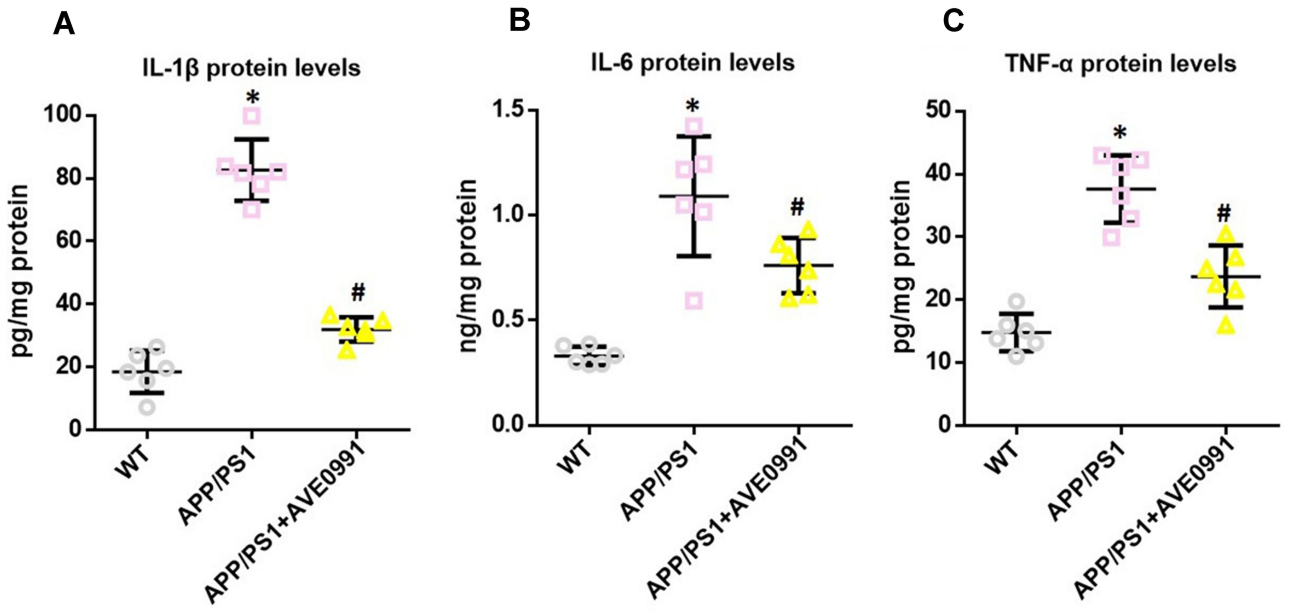

Figure 2 AVE0991 suppresses neuroinflammation in APP/PS1 mice. (**A**–**C**) ELISA assay of IL-1β, IL-6 and TNF-α protein in the brain (n=6 per group). All data are expressed as the mean ± SD. *P<0.05 versus the WT group. #P<0.05 versus the APP/PS1 group.

were identified with the threshold of corrected P<0.001 and |log2FC>1| after AVE0991 treatment. Among them, one lncRNA was significantly upregulated whilst the other 30 lncRNAs were markedly downregulated. SNHG14 was revealed to be the most downregulated lncRNA following AVE0991 treatment. This alteration of SNHG14 levels in primary astrocytes from APP/PS1 mice after AVE0991 was further validated by qRT-PCR (Figure 3D).

AVE0991 Inhibits the Expression of NLRP3 Inflammasome in Primary Astrocytes by a SNHG14-Dependent Manner

Next, we employed primary astrocytes from WT neonatal mice to confirm this finding. As indicated by Figure 4A, $A\beta_{1\text{-}42}$ significantly upregulated SNHG14 expression, and this upregulation was attenuated by AVE0991. To test whether AVE0991 inhibited astrocytic NLRP3 inflammasome via a SNHG14-dependent manner, a CRISPR-dCAS9-SAM-mediated lentiviral strategy was used to overexpress SNHG14 in mouse primary astrocytes (Supplementary Figure S4). The AVE0991-induced downregulation of NLRP3 protein levels was reversed by SNHG14 overexpression (Figure 4B and C). Meanwhile, overexpression of SNHG14 abolished the decrement of IL-1β protein levels caused by AVE0991 in the culture medium (Figure 4D).

SNHG14 Acts as a Sponge of miR-223-3p While NLRP3 is a Direct Target of miR-223-3p

The cellular location is important for the biological functions of lncRNAs.[27] Therefore, FISH was employed to determine the subcellular localization of SNHG14 in the astrocyte of 8-month-old APP/PS1 mice. As revealed by Supplementary Figure S5, SNHG14 was expressed predominantly in the cytoplasm of astrocyte. Since lncRNAs in the cytoplasm were reported to downregulate gene expression by sponging specific miRNAs,[28] it is possible that SNHG14 may function as a miRNA sponge and thus regulates NLRP3 expression at the post-transcriptional.

We then used online bioinformatics databases to screen potential miRNAs that can bind to both SNHG14 and the 3′-UTR of NLRP3, and miR-223-3p was initially identified. To confirm the direct binding between SNHG14 and miR-223-3p, dual-luciferase reporter assay was conducted in HEK 293T cells. As expected, miR-223-3p significantly reduced the SNHG14-WT luciferase activity, but not that of SNHG14-Mut (Figure 5A and B). To further evaluate the interaction between SNHG14 and miR-223-3p, we manipulated SNHG14 levels in primary astrocytes from WT neonatal mice (Supplementary Figure S6). As revealed by Figure 5C, SNHG14 overexpression significantly reduced miR-223-3p levels whilst knockdown of SNHG14 marked elevated miR-223-3p levels. Next, dual-

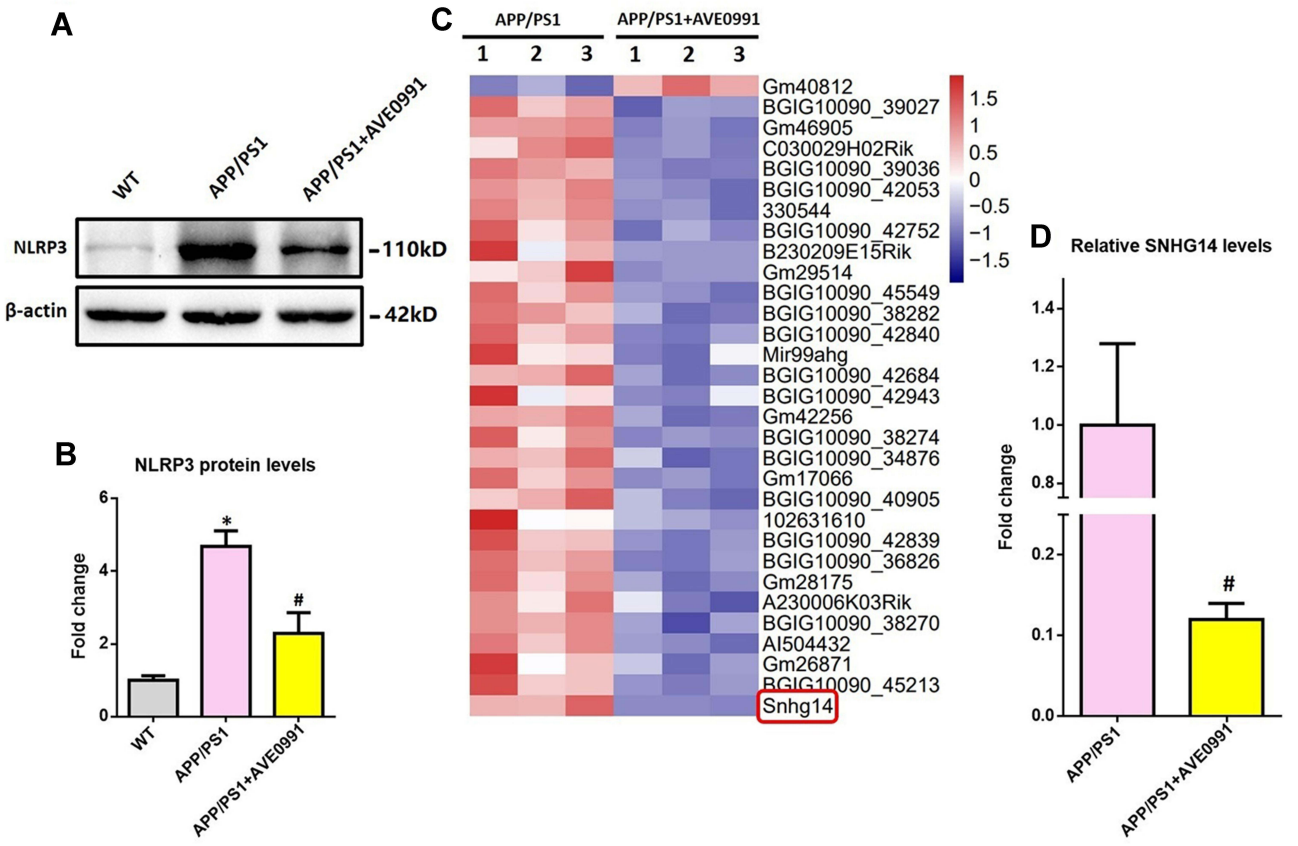

Figure 3 LncRNA SNHG14 might be involved in the AVE0991-induced inhibition of astrocytic NLRP3 inflammasome. (**A** and **B**) Representative Western blot bands and densitometric analysis of NLRP3 in the brain (n=6 per group). β-Actin was used as an internal control. (**C**) The heatmap represents hierarchical clustering for differentially expressed lncRNAs in the astrocytes from adult mice (n=3 per group). (**D**) The qRT-PCR result of SNHG14 expression in the primary astrocytes from adult mice (n=3 per group). All data are expressed as the mean ± SD. *P<0.05 versus the WT group. #P<0.05 versus the APP/PS1 group.

luciferase reporter assay was conducted in HEK 293T cells to validate whether NLRP3 is a direct target of miR-223-3p. As demonstrated by Figure 5D and E, miR-223-3p markedly inhibited NLRP3-3′-UTR-WT luciferase activity, but not that of NLRP3-3′-UTR-Mut.

miR-223-3p Participates in the AVE0991-Induced Suppression of Astrocytic NLRP3 Inflammasome

Lastly, we investigated whether miR-223-3p participated in the AVE0991-induced astrocytic NLRP3 inflammasome suppression. As revealed by Figure 6A, $A\beta_{1\text{-}42}$ significantly reduced miR-223-3p expression, and this reduction was reversed by AVE0991. Meanwhile, miR-223-3p inhibitor reversed the AVE0991-induced downregulation of NLRP3 protein levels (Figure 6B and C). The decrement of IL-1β protein levels caused by AVE0991 in the culture medium was also abolished by miR-223-3p inhibitor (Figure 6D).

Discussion

As a newly identified component of RAS, Ang-(1–7) was revealed to improve cognitive functions in animal models of AD.[29–31] However, Ang-(1–7) has a relatively short duration of biological effect in vivo since it can be rapidly inactivated and degraded by several proteases.[17] Therefore, a nonpeptide Ang-(1–7) analogue AVE0991 was employed in this study. Intraperitoneal injection of AVE0991 rescues cognitive impairments in APP/PS1 mice. To our knowledge, this is the first study revealing a beneficial effect of AVE0991 on cognitive functions in AD animal models. This might be attributed to the neuroprotective effects of AVE0991, since neuronal and synaptic losses in the brain of APP/PS1 mice were rescued by AVE0991 treatment. This finding was in accordance with our previous observations that AVE0991 prevented neuronal and synaptic degeneration in a rat model of vascular dementia.[19] It should be noted that our results did not support a direct involvement of

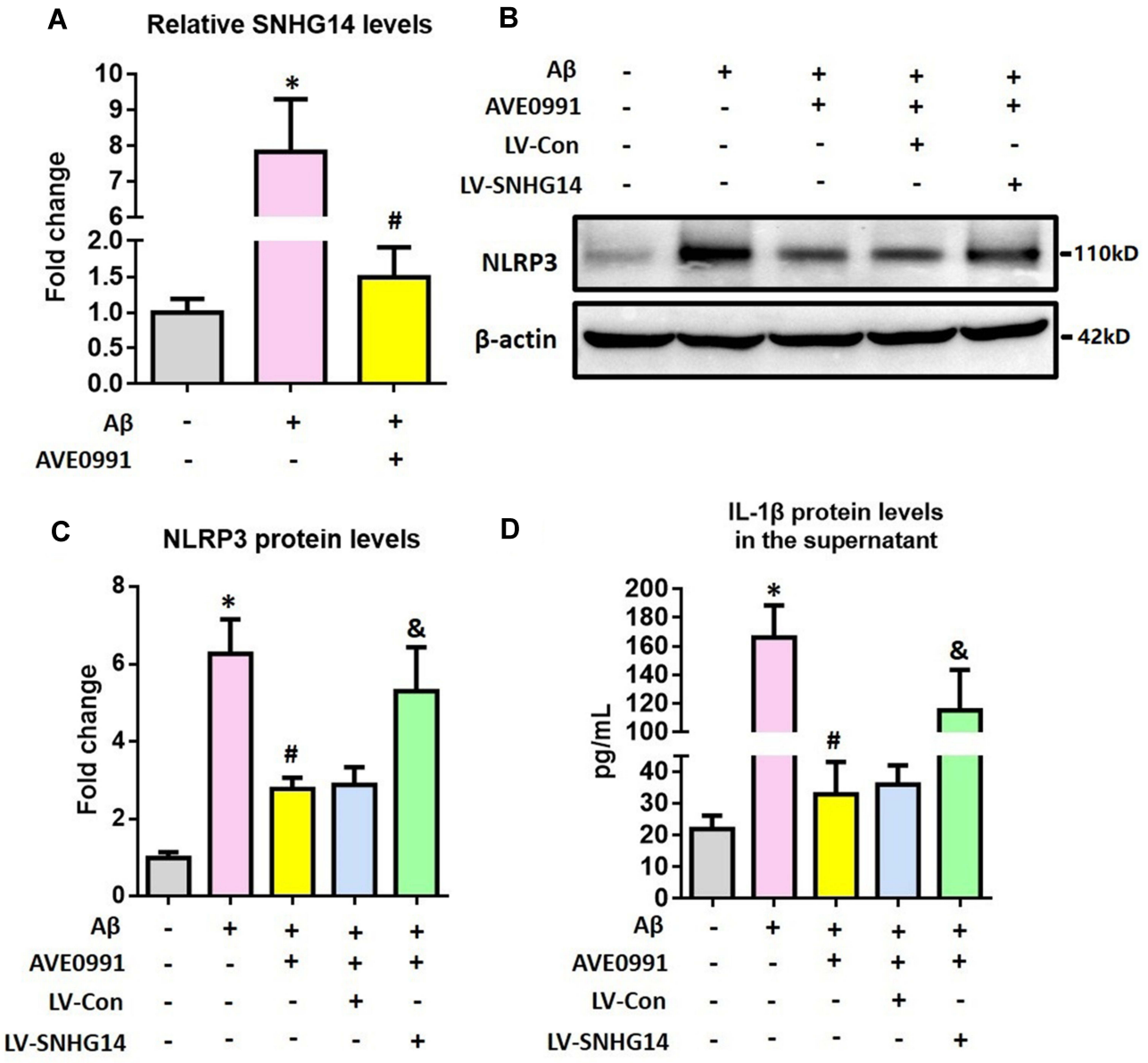

Figure 4 AVE0991 inhibits astrocytic NLRP3 inflammasome via a SNHG14-dependent manner. (**A**) The qRT-PCR result of SNHG14 expression in the primary astrocytes following $A\beta_{1\text{-}42}$ stimulation. (**B** and **C**) Representative Western blot bands and densitometric analysis of NLRP3 in the primary astrocytes. β-Actin was used as an internal control. (**D**) ELISA assay of IL-1β protein in the culture medium of primary astrocytes. All data are expressed as the mean ± SD of 3 independent experiments. *P<0.05 versus the NC group. #P<0.05 versus the Aβ group. &P<0.05 versus the Aβ+AVE0991+LV-Con group.

AVE0991 in cognitive enhancement, since AVE0991 has no influence on spatial cognitive performance of WT mice in MWM test. This appears to contradict previous observations that Ang-(1–7) might possess a direct cognitive enhancement property.[32] This discrepancy might be ascribed to the difference in administration route (intraperitoneal injection versus intracerebral injection) and dosage.

In this study, pro-inflammatory cytokines were reduced in the brain of APP/PS1 mice following AVE0991 treatment, indicating an anti-inflammatory effect of AVE0991. The anti-inflammatory effect of AVE0991 has been confirmed in experimental models of arthritis, atherosclerosis, chronic asthma, and the heatstroke-induced liver damage.[33–36] Since neuroinflammation leads to the neuronal and synaptic damages under AD conditions, the AVE0991-mediated neuroprotection might be attributed to its anti-inflammatory actions.

Emerging evidence suggested that astrocyte, the most abundant type of cells within the brain, regulates

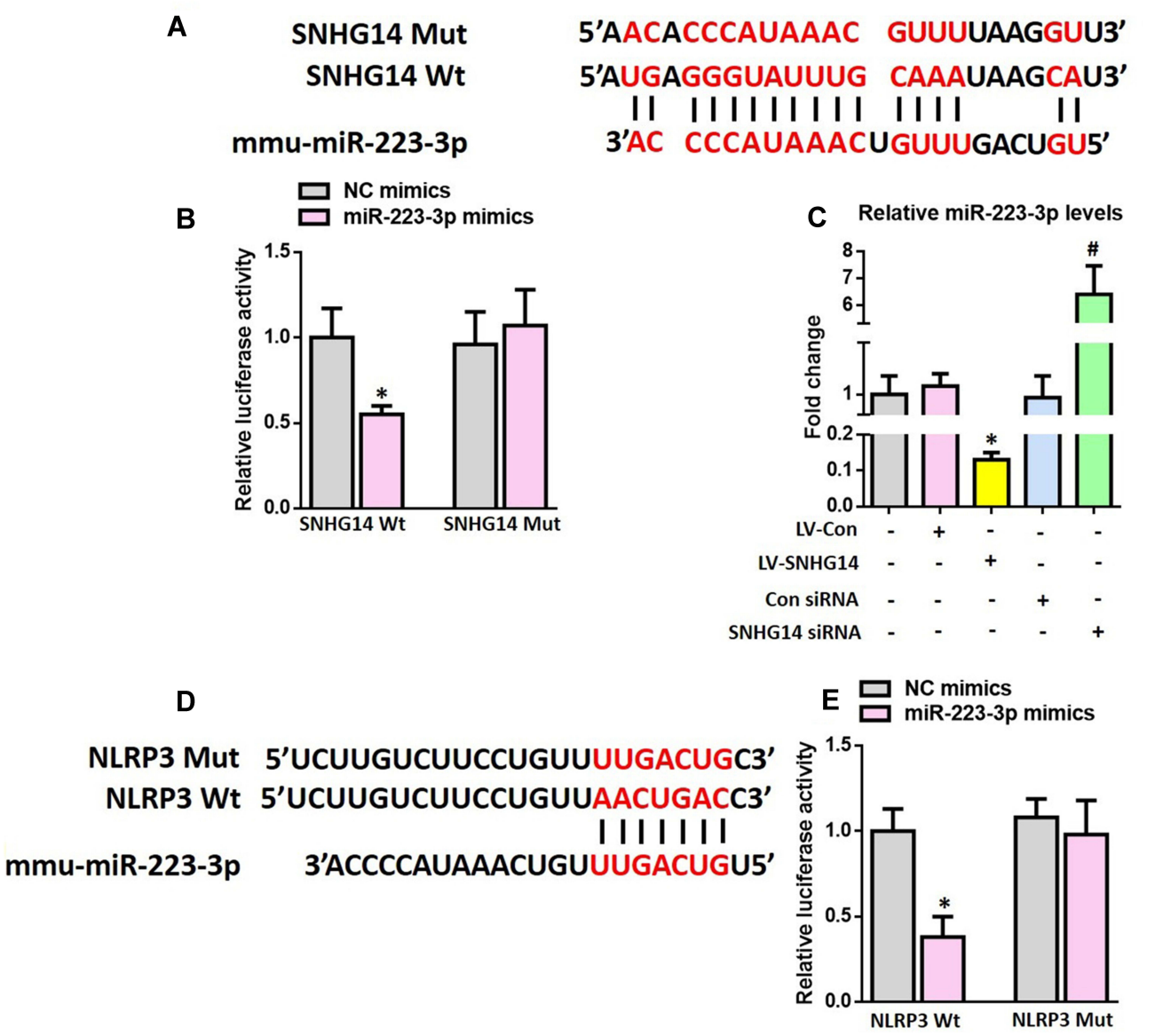

Figure 5 SNHG14 acts as a sponge of miR-223-3p while NLRP3 is a direct target of miR-223-3p. (**A**) The predicted binding sites between SNHG14 and miR-223-3p. (**B**) Luciferase reporter assay in HEK 293T cells transfected with psiCHECK2-SNHG14 (WT or Mut) and miR-223-3p mimics or NC mimics. (**C**) The qRT-PCR result of miR-223-3p expression in the primary astrocytes after modulation of SNHG14 expression. (**D**) The predicted binding sites between miR-223-3p and the 3′-UTR of NLRP3. (**E**) Luciferase reporter assay in HEK 293T cells transfected with psiCHECK2-NLRP3 (WT or Mut) and miR-223-3p mimics or NC mimics. All data are expressed as the mean ± SD of 3 independent experiments. **P*<0.05 versus the NC mimics or LV-Con group. #*P*<0.05 versus the Con siRNA group.

neuroinflammation under AD condition.[12] Interestingly, MAS1 receptor is highly expressed on the surface of astrocytes whilst NLRP3 inflammasome was identified within astrocytes.[13,25] The NLRP3 inflammasome is composed of NLRP3, ASC, and procaspase-1.[37] Activation of NLRP3 inflammasome converts the inactive pro-IL-1β into its active form and thus mediates the subsequent inflammatory response.[37] Accumulating evidence indicated that NLRP3 inflammasome activation contributed to the pathogenesis of AD by eliciting brain inflammatory response.[26] Meanwhile, inhibition of NLRP3 inflammasome might represent a new therapeutic intervention for this disease.[38] In the current study, the NLRP3 levels in the primary astrocytes from AVE0991-treated APP/PS1 mice were significantly lower than those from APP/PS1 mice without AVE0991 treatment, indicating a suppression of NLRP3 inflammasome caused by AVE0991. Therefore, it seemed that the anti-inflammatory effects of AVE0991 might be achieved by suppressing astrocytic NLRP3 inflammasome.

LncRNAs represent a subgroup of RNAs lacking protein-coding capacity.[39] Recently, lncRNAs were revealed

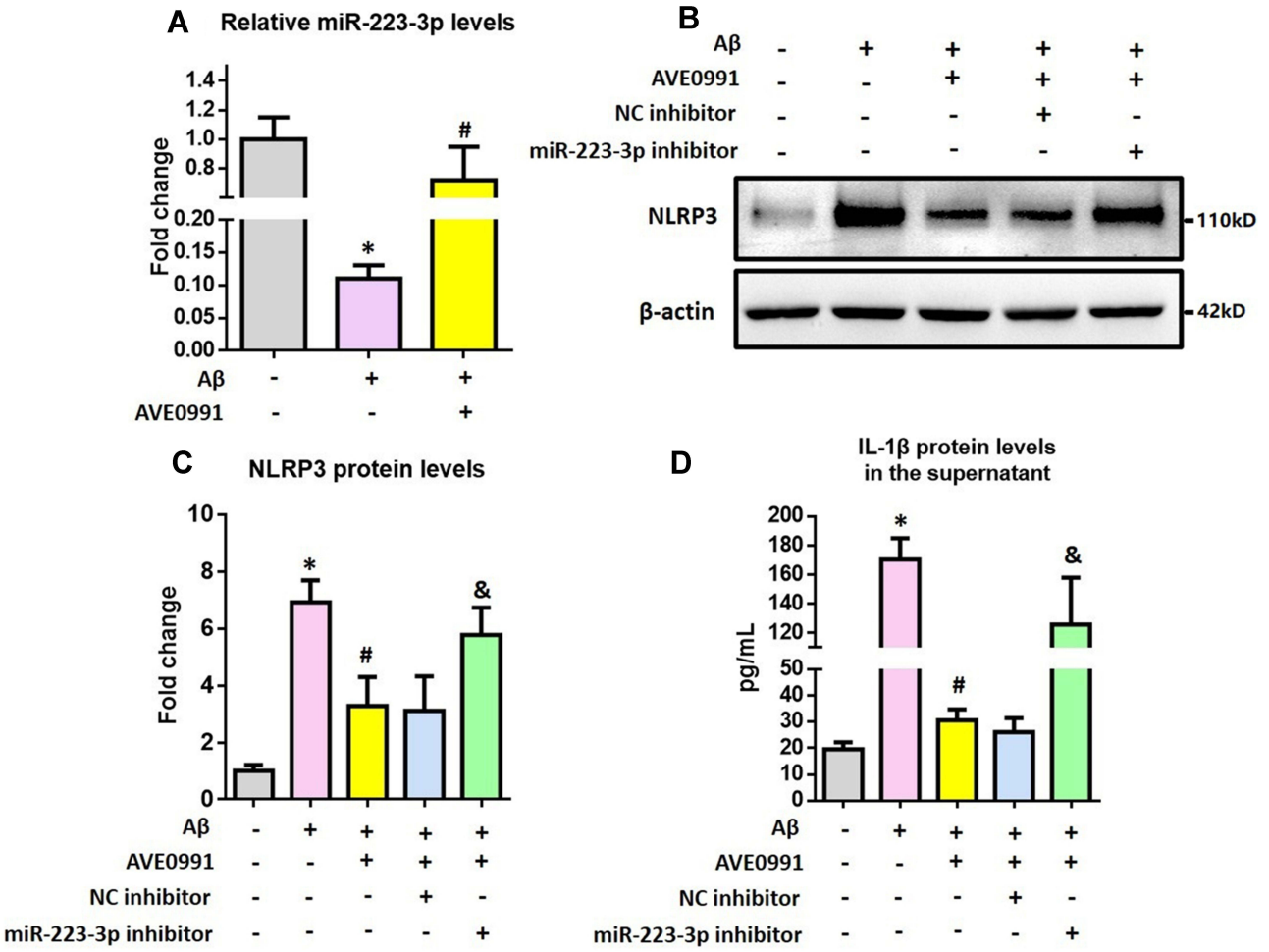

Figure 6 miR-223-3p participates in the AVE0991-induced suppression of astrocytic NLRP3 inflammasome. (**A**) The qRT-PCR result of miR-223-3p expression in the primary astrocytes. (**B** and **C**) Representative Western blot bands and densitometric analysis of NLRP3 in the primary astrocytes. β-Actin was used as an internal control. (**D**) ELISA assay of IL-1β protein in the culture medium of primary astrocytes. All data are expressed as the mean ± SD of 3 independent experiments. **P*<0.05 versus the NC group. #*P*<0.05 versus the Aβ group. &*P*<0.05 versus the Aβ+AVE0991+NC inhibitor group.

to play an important role in modulating neuroinflammation and thus contributed to the pathogenesis of numerous neurological diseases including ischemic stroke, cerebral hemorrhage, epilepsy, Parkinson's disease, and Alzheimer's disease.[40–44] Based on this evidence, we then asked whether lncRNAs were involved in the AVE0991-induced inhibition of astrocytic NLRP3 inflammasome. High-throughput lncRNA sequencing and qRT-PCR validation indicated that SNHG14 was the most downregulated lncRNA in astrocytes from AVE0991-treated APP/PS1 mice. In vitro, the Aβ-induced upregulation of SNHG14 was suppressed by AVE0991 while SNHG14 overexpression reversed the AVE0991-induced suppression of NLRP3 inflammasome. This observation indicated that AVE0991 inhibited astrocytic NLRP3 inflammasome via a SNHG14-dependent manner.

Mounting evidence indicated that the cellular location is important for the biological functions of lncRNAs.[27] Here, we found that SNHG14 was more abundant in the cytoplasm of astrocyte. Previous studies reported that lncRNAs in the cytoplasm could downregulate gene expression by sponging specific miRNAs.[28] In view of this evidence, we speculated that SNHG14 might function as a miRNA sponge and thus regulated NLRP3 expression at the post-transcriptional level in astrocytes. Using online bioinformatics databases, we revealed that miR-223-3p not only target NLRP3 but also have SNHG14 binding sites. The interaction between SNHG14 and miR-223-3p was validated by dual-luciferase reporter assay while the levels of miR-223-3p were negatively regulated by SNHG14, indicating that SNHG14 sponges miR-223-3p. To our knowledge, this is the first study reporting that SNHG14 act as an endogenous sponge

of miR-223-3p. Moreover, dual-luciferase reporter assay also confirmed the binding between miR-223-3p and NLRP3. This finding was consistent with previous observations that NLRP3 is a direct target of miR-223-3p.[45,46]

Lastly, we revealed that miR-223-3p levels in the astrocytes were upregulated by AVE0991 while miR-223-3p inhibitor reversed the AVE0991-induced suppression of NLRP3 inflammasome. This finding indicated that miR-223-3p participated in the AVE0991-induced suppression of astrocytic NLRP3 inflammasome.

Some minor issues should be mentioned here. In addition to astrocyte, microglia participated in the pathogenesis of AD by eliciting NLRP3 inflammasome-mediated neuroinflammation either. Meanwhile, the Ang-(1–7) receptor MAS1 was identified on microglia. Therefore, it is also possible that the neuroprotection of Ang-(1–7) under AD condition may be partly achieved by suppression of microglial NLRP3 inflammasome-mediated neuroinflammation. In our future studies, this speculation will be tested and the potential molecular mechanisms will be investigated.

In summary, this study suggested that Ang-(1–7) analogue AVE0991 inhibited astrocyte-mediated neuroinflammation via SNHG14/miR-223-3p/NLRP3 pathway and offered neuroprotection in APP/PS1 mice. These findings reveal the underlying mechanisms by which Ang-(1–7) modulates neuroinflammation under AD condition and uncover the potential of its nonpeptide analogue AVE0991 in AD treatment.

Funding

This work was supported by the National Natural Science Foundation of China (81771140), Natural Science Foundation of Jiangsu Province (BK20201117), and Jiangsu "Six One Project" for Distinguished Medical Scholars (LGY2020013).

Disclosure

The authors declare that there is no conflict of interest.

References

1. Jiang T, Yu JT, Tian Y, Tan L. Epidemiology and etiology of alzheimer's disease: from genetic to non- genetic factors. *Curr Alzheimer Res*. 2013;10(8):852–867. doi:10.2174/15672050113109990155
2. Leng F, Edison P. Neuroinflammation and microglial activation in Alzheimer disease: where do we go from here? *Nat Rev Neurol*. 2021;17(3):157–172. doi:10.1038/s41582-020-00435-y
3. Brod SA. Anti-inflammatory agents: an approach to prevent cognitive decline in alzheimer's disease. *J Alzheimer's Dis*. 2021;1–16. doi:10.3233/JAD-215125
4. Schweda F. Salt feedback on the renin-angiotensin-aldosterone system. *Pflugers Archiv*. 2015;467(3):565–576. doi:10.1007/s00424-014-1668-y
5. Loera-Valencia R, Eroli F, Garcia-Ptacek S, Maioli S. Brain renin-angiotensin system as novel and potential therapeutic target for alzheimer's disease. *Int J Mol Sci*. 2021;22(18):10139. doi:10.3390/ijms221810139
6. Xu P, Sriramula S, Lazartigues E. ACE2/ANG-(1-7)/Mas pathway in the brain: the axis of good. research support, N.I.H., extramural review. *Am J Physiol Regul Integr Comp Physiol*. 2011;300(4):R804–17. doi:10.1152/ajpregu.00222.2010
7. Santos RA, Simoes e Silva AC, Maric C, et al. Angiotensin-(1-7) is an endogenous ligand for the G protein-coupled receptor Mas. Research Support, Non-U.S. Gov't. *Proc Natl Acad Sci U S A*. 2003;100(14):8258–8263. doi:10.1073/pnas.1432869100
8. Jiang T, Tan L, Gao Q, et al. Plasma Angiotensin-(1-7) is a potential biomarker for alzheimer's disease. *Curr Neurovasc Res*. 2016;13(2):96–99. doi:10.2174/1567202613666160224124739
9. Jiang T, Xue LJ, Yang Y, et al. AVE0991, a nonpeptide analogue of Ang-(1-7), attenuates aging-related neuroinflammation. *Aging*. 2018;10(4):645–657. doi:10.18632/aging.101419
10. Jiang T, Zhang YD, Zhou JS, et al. Angiotensin-(1-7) is reduced and inversely correlates with tau hyperphosphorylation in animal models of alzheimer's disease. *Mol Neurobiol*. 2016;53(4):2489–2497. doi:10.1007/s12035-015-9260-9
11. Duan R, Xue X, Zhang QQ, et al. ACE2 activator diminazene aceturate ameliorates Alzheimer's disease-like neuropathology and rescues cognitive impairment in SAMP8 mice. *Aging*. 2020;12(14):14819–14829. doi:10.18632/aging.103544
12. Kwon HS, Koh SH. Neuroinflammation in neurodegenerative disorders: the roles of microglia and astrocytes. *Transl Neurodegener*. 2020;9(1):42. doi:10.1186/s40035-020-00221-2
13. Moore ED, Kooshki M, Metheny-Barlow LJ, Gallagher PE, Robbins ME. Angiotensin-(1-7) prevents radiation-induced inflammation in rat primary astrocytes through regulation of MAP kinase signaling. *Free Radic Biol Med*. 2013;65:1060–1068. doi:10.1016/j.freeradbiomed.2013.08.183
14. Chen Z, Wu H, Zhang M. Long non-coding RNA: an underlying bridge linking neuroinflammation and central nervous system diseases. *Neurochem Int*. 2021;148:105101. doi:10.1016/j.neuint.2021.105101
15. Xie W, Wu D, Ren Y, et al. OIP5-AS1 attenuates microangiopathy in diabetic mouse by regulating miR-200b/ACE2. *World Neurosurg*. 2020;139:e52–e60. doi:10.1016/j.wneu.2020.03.063
16. Li W, Wang R, Ma JY, et al. A human long non-coding RNA ALT1 controls the cell cycle of vascular endothelial cells via ACE2 and cyclin D1 pathway. *Cell Physiol Biochem*. 2017;43(3):1152–1167. doi:10.1159/000481756
17. Vickers C, Hales P, Kaushik V, et al. Hydrolysis of biological peptides by human angiotensin-converting enzyme-related carboxypeptidase. *J Biol Chem*. 2002;277(17):14838–14843. doi:10.1074/jbc.M200581200
18. Jiang T, Tan L, Zhu XC, et al. Upregulation of TREM2 ameliorates neuropathology and rescues spatial cognitive impairment in a transgenic mouse model of Alzheimer's disease. *Neuropsychopharmacology*. 2014;39(13):2949–2962. doi:10.1038/npp.2014.164
19. Xue X, Duan R, Zhang QQ, et al. A non-peptidic MAS1 agonist AVE0991 alleviates hippocampal synaptic degeneration in rats with chronic cerebral hypoperfusion. *Curr Neurovasc Res*. 2021;18. doi:10.2174/1567202618666211012095210
20. Larson ME, Lesne SE. Soluble Abeta oligomer production and toxicity. Research Support, N.I.H., Extramural Research Support, Non-U.S. Gov't Review. *J Neurochem*. 2012;120 Suppl 1:125–139. doi:10.1111/j.1471-4159.2011.07478.x

21. Livak KJ, Schmittgen TD. Analysis of relative gene expression data using real-time quantitative PCR and the 2(-Delta Delta C(T)) Method. *Methods*. 2001;25(4):402–408. doi:10.1006/meth.2001.1262
22. Kim D, Langmead B, Salzberg SL. HISAT: a fast spliced aligner with low memory requirements. *Nat Methods*. 2015;12(4):357–360. doi:10.1038/nmeth.3317
23. Love MI, Huber W, Anders S. Moderated estimation of fold change and dispersion for RNA-seq data with DESeq2. *Genome Biol*. 2014;15(12):550. doi:10.1186/s13059-014-0550-8
24. Yang CC, Lin CC, Hsiao LD, Kuo JM, Tseng HC, Yang CM. Lipopolysaccharide-induced matrix metalloproteinase-9 expression associated with cell migration in rat brain astrocytes. *Int J Mol Sci*. 2019;21(1). doi:10.3390/ijms21010259
25. Zhu J, Hu Z, Han X, et al. Dopamine D2 receptor restricts astrocytic NLRP3 inflammasome activation via enhancing the interaction of beta-arrestin2 and NLRP3. *Cell Death Differ*. 2018;25 (11):2037–2049. doi:10.1038/s41418-018-0127-2
26. Heneka MT, Kummer MP, Stutz A, et al. NLRP3 is activated in Alzheimer's disease and contributes to pathology in APP/PS1 mice. *Nature*. 2013;493(7434):674–678. doi:10.1038/nature11729
27. Jin Y, Zhang M, Duan R, et al. Long noncoding RNA FGF14-AS2 inhibits breast cancer metastasis by regulating the miR-370-3p/FGF14 axis. *Cell Death Discov*. 2020;6:103. doi:10.1038/s41420-020-00334-7
28. Tay Y, Rinn J, Pandolfi PP. The multilayered complexity of ceRNA crosstalk and competition. *Nature*. 2014;505(7483):344–352. doi:10.1038/nature12986
29. Evans CE, Miners JS, Piva G, et al. ACE2 activation protects against cognitive decline and reduces amyloid pathology in the Tg2576 mouse model of Alzheimer's disease. *Acta Neuropathol*. 2020;139 (3):485–502. doi:10.1007/s00401-019-02098-6
30. Cao C, Hasegawa Y, Hayashi K, Takemoto Y, Kim-Mitsuyama S. Chronic angiotensin 1-7 infusion prevents angiotensin-ii-induced cognitive dysfunction and skeletal muscle injury in a mouse model of alzheimer's disease. *J Alzheimer's Dis*. 2019;69(1):297–309. doi:10.3233/JAD-181000
31. Uekawa K, Hasegawa Y, Senju S, et al. Intracerebroventricular infusion of angiotensin-(1-7) ameliorates cognitive impairment and memory dysfunction in a mouse model of alzheimer's disease. *J Alzheimer's Dis*. 2016;53(1):127–133. doi:10.3233/JAD-150642
32. Ho JK, Nation DA. Cognitive benefits of angiotensin IV and angiotensin-(1-7): a systematic review of experimental studies. *Neurosci Biobehav Rev*. 2018;92:209–225. doi:10.1016/j.neubiorev.2018.05.005
33. da Silveira KD, Coelho FM, Vieira AT, et al. Anti-inflammatory effects of the activation of the angiotensin-(1-7) receptor, MAS, in experimental models of arthritis. *J Immunol*. 2010;185 (9):5569–5576. doi:10.4049/jimmunol.1000314
34. Jawien J, Toton-Zuranska J, Gajda M, et al. Angiotensin-(1-7) receptor Mas agonist ameliorates progress of atherosclerosis in apoE-knockout mice. *J Physiol Pharmacol*. 2012;63(1):77–85.
35. Rodrigues-Machado MG, Magalhaes GS, Cardoso JA, et al. AVE 0991, a non-peptide mimic of angiotensin-(1-7) effects, attenuates pulmonary remodelling in a model of chronic asthma. *Br J Pharmacol*. 2013;170(4):835–846. doi:10.1111/bph.12318
36. Zhang M, Zhu X, Tong H, et al. AVE 0991 attenuates pyroptosis and liver damage after heatstroke by inhibiting the ROS-NLRP3 inflammatory signalling pathway. *Biomed Res Int*. 2019;2019:1806234. doi:10.1155/2019/1806234
37. Tan MS, Yu JT, Jiang T, Zhu XC, Tan L. The NLRP3 inflammasome in Alzheimer's disease. *Mol Neurobiol*. 2013;48(3):875–882. doi:10.1007/s12035-013-8475-x
38. Kuwar R, Rolfe A, Di L, et al. A novel inhibitor targeting NLRP3 inflammasome reduces neuropathology and improves cognitive function in alzheimer's disease transgenic mice. *J Alzheimer's Dis*. 2021;82(4):1769–1783. doi:10.3233/JAD-210400
39. Oo JA, Brandes RP, Leisegang MS. Long non-coding RNAs: novel regulators of cellular physiology and function. *Pflugers Archiv*. 2021. doi:10.1007/s00424-021-02641-z
40. Yan H, Rao J, Yuan J, et al. Long non-coding RNA MEG3 functions as a competing endogenous RNA to regulate ischemic neuronal death by targeting miR-21/PDCD4 signaling pathway. *Cell Death Dis*. 2017;8(12):3211. doi:10.1038/s41419-017-0047-y
41. Li JW, Ren SH, Ren JR, et al. Nimodipine improves cognitive impairment after subarachnoid hemorrhage in rats through lncRNA NEAT1/miR-27a/MAPT axis. *Drug Des Devel Ther*. 2020;14:2295–2306. doi:10.2147/DDDT.S248115
42. Han CL, Ge M, Liu YP, et al. Long non-coding RNA H19 contributes to apoptosis of hippocampal neurons by inhibiting let-7b in a rat model of temporal lobe epilepsy. *Cell Death Dis*. 2018;9(6):617. doi:10.1038/s41419-018-0496-y
43. Lv K, Liu Y, Zheng Y, Dai S, Yin P, Miao H. Long non-coding RNA MALAT1 regulates cell proliferation and apoptosis via miR-135b-5p/GPNMB axis in Parkinson's disease cell model. *Biol Res*. 2021;54 (1):10. doi:10.1186/s40659-021-00332-8
44. Zhang YY, Bao HL, Dong LX, Liu Y, Zhang GW, An FM. Silenced lncRNA H19 and up-regulated microRNA-129 accelerates viability and restrains apoptosis of PC12 cells induced by Aβ in a cellular model of Alzheimer's disease. *Cell Cycle*. 2021;20(1):112–125. doi:10.1080/15384101.2020.1863681
45. Wu ZM, Luo J, Shi XD, Zhang SX, Zhu XB, Guo J. Icariin alleviates rheumatoid arthritis via regulating miR-223-3p/NLRP3 signalling axis. *Autoimmunity*. 2020;53(8):450–458. doi:10.1080/08916934.2020.1836488
46. Chen L, Hou X, Zhang M, et al. MicroRNA-223-3p modulates dendritic cell function and ameliorates experimental autoimmune myocarditis by targeting the NLRP3 inflammasome. *Mol Immunol*. 2020;117:73–83. doi:10.1016/j.molimm.2019.10.027